



1 A multi-year observation of nitrous oxide at the Boknis Eck 2 Time-Series Station in the Eckernförde Bay (southwestern 3 Baltic Sea)

4 Xiao Ma¹, Sinikka T. Lennartz^{1,2}, and Hermann W. Bange¹

5 ¹ GEOMAR Helmholtz Centre for Ocean Research Kiel, Düsternbrooker Weg 20, 24105 Kiel, Germany

6 ² now at ICBM, University of Oldenburg, Oldenburg, Germany

7 Correspondence to: Xiao Ma (mxiao@geomar.de)

8

9 **Abstract.** Nitrous oxide (N₂O) is a potent greenhouse gas and it is involved in stratospheric ozone
10 depletion. Its oceanic production is mainly influenced by dissolved nutrient and oxygen (O₂)
11 concentrations in the water column. Here we examined the seasonal and annual variations of
12 dissolved N₂O at the Boknis Eck (BE) Time-Series Station located in Eckernförde Bay
13 (southwestern Baltic Sea). Monthly measurements of N₂O started in July 2005. We found a
14 pronounced seasonal pattern for N₂O with high concentrations (supersaturations) in winter/early
15 spring and low concentrations (undersaturations) in autumn when hypoxic/anoxic conditions
16 prevail. Unusually low N₂O concentrations were observed during October 2016–April 2017,
17 which was presumably a result of prolonged anoxia and the subsequent nutrient deficiency.
18 Unusually high N₂O concentrations were found in November 2017 and this event was linked to
19 the occurrence of upwelling which interrupted N₂O consumption via denitrification and
20 potentially promoted ammonium oxidation (nitrification) at the oxic/anoxic interface. Nutrient
21 concentrations (such as nitrate, nitrite and phosphate) at BE are decreasing since 1980s, but
22 oxygen concentrations in the water column are still decreasing. Our results indicate a close
23 coupling of N₂O anomalies to O₂ concentration, nutrients and stratification. Given the long-term
24 trends of declining nutrient and oxygen concentrations at BE, a decrease in N₂O concentration,
25 and thus emissions, seems likely due to an increasing number of events with low N₂O
26 concentrations.

27 1. Introduction

28 Long-term observation with regular measurement intervals can be an effective way to monitor
29 seasonal and interannual variabilities as well as to decipher short- and long-term trends of an
30 ecosystem, which are required to make projections of the future ecosystem development (see e.g.
31 Ducklow et al., 2009). Recently, multi-year time-series measurements of nitrous oxide (N₂O), a
32 potent greenhouse gas and a major threat to ozone depletion (IPCC, 2013; Ravishankara et al.,
33 2009), have been reported from the coastal upwelling areas off central Chile (Farías et al., 2015)
34 and off Goa (Naqvi et al., 2010), in the North Pacific Subtropical Gyre (Wilson et al., 2017), and
35 in Saanich Inlet (Capelle et al., 2018).



36 N₂O production in the ocean is generally dominated by microbial nitrification (NH₄⁺ → NO₂⁻ →
37 NO₃⁻) and denitrification (NO₃⁻ → NO₂⁻ → N₂O → N₂). During bacterial/archaeal nitrification,
38 N₂O is produced as a by-product with enhanced N₂O production under low oxygen (O₂)
39 conditions (e.g. Goreau et al., 1980; Löscher et al., 2012). N₂O is produced as an intermediate
40 during bacterial denitrification (Codispoti et al., 2005). N₂O could be further consumed via
41 denitrification to dinitrogen, however, this process is inhibited with the presence of O₂ because
42 of the low O₂ tolerance of the enzyme involved (Bonin et al. 1989). This incomplete pathway is
43 called partial denitrification and can lead to N₂O accumulation (e.g. Naqvi et al., 2000; Farías et
44 al., 2009).

45 The oceans including coastal areas contribute ~25% of the natural and anthropogenic N₂O
46 emissions (IPCC, 2013), with disproportionately high emissions from coastal and estuarine areas
47 (Bange, 2006). N₂O emissions from coastal areas strongly depend on nitrogen inputs (Seitzinger
48 and Kroeze, 1998; Zhang et al., 2010). The increasing input of nitrogen (i.e. eutrophication) has
49 become a worldwide problem in coastal waters leading to enhanced productivity and severe O₂
50 depletion caused by enhanced degradation of organic matter (Breitburg et al., 2017; Rabalais et
51 al., 2014). The decline in O₂ concentration (i.e. deoxygenation), either in coastal waters or the
52 open ocean, might result in favorable conditions for N₂O production (Codispoti et al., 2001;
53 Nevison et al., 2003). The results of a model study by Kroeze and Seitzinger (1998) indicated a
54 significant increase of N₂O in European coastal waters for 2050. Moreover, it has been suggested
55 that N₂O production and emissions are very likely to increase in the near future, especially in the
56 shallow suboxic/anoxic coastal systems (Naqvi et al., 2000; Bange, 2006). However, model
57 projections show a net decrease in future global oceanic N₂O emission during the 21st century
58 (Martinez-Rey et al., 2015; Landolfi et al., 2017; Battaglia and Joos, 2018).

59 The Baltic Sea is a nearly enclosed, marginal sea with a very limited access to the open ocean via
60 the North Sea. The restricted water exchange with the North Sea and extensive human activities,
61 such agriculture, industrial production and sewage discharge in the catchment area led to high
62 inputs of nutrients to the Baltic Sea. As a result, the areas affected by anoxia have been
63 expanding in the deep basins of the central Baltic Sea (Carstensen et al., 2014). In order to
64 control this situation, the Helsinki Commission (HELCOM) was established in 1974 and a series
65 of measures have been taken to prevent anthropogenic nutrient input into the Baltic Sea.
66 Consequently, the nutrient inputs (by riverine loads, direct point-sources and, for nitrogen,
67 atmospheric deposition) to the Baltic Sea are declining (HELCOM, 2018a). However, the
68 number of low O₂ (i.e. hypoxic/anoxic) events in coastal waters of the Baltic Sea is increasing
69 and deoxygenation is still going on (Conley et al., 2011; Lennartz et al., 2014). The
70 deoxygenation in the Baltic Sea can affect the production/consumption of N₂O. Our group has
71 been monitoring dissolved N₂O concentrations at the Boknis Eck Time-Series Station, located in
72 Eckernförde Bay (southwestern Baltic Sea), for more than a decade. In this study, we present
73 monthly measurements of N₂O and biogeochemical parameters such as nutrients and O₂ from
74 July 2005 to December 2017. The major objectives of our study were: 1) to decipher the seasonal



75 pattern of N₂O distribution in the water column, 2) to identify short-term and long-term trends of
76 the N₂O concentrations, 3) to explore the potential role of nutrients and O₂ for N₂O
77 production/consumption, and 4) to quantify the sea-to-air N₂O flux density at the time-series
78 station.

79 **2. Material and methods**

80 **2.1 Study site**

81 Sampling at the Boknis Eck (BE) Time-Series Station (www.bokniseck.de) started on 30 April
82 1957 and, therefore, it is one of the oldest continuously operated time-series stations in the world.
83 The BE station is located at the entrance of the Eckernförde Bay (54°31' N, 10°02' E, Fig. 1) in
84 the southwestern Baltic Sea. The water depth of the sampling site is 28 m. Various physical,
85 chemical and biological parameters are measured on a monthly basis (Lennartz et al., 2014).
86 There is no significant river runoff to Eckernförde Bay and the saline North Sea water inflow
87 from the Kattegat plays a dominant role for the local hydrographic conditions. Seasonal
88 stratification usually starts to develop in April and lasts until October, during which hypoxia or
89 even anoxia (characterized by the presence of hydrogen sulphide, H₂S) sporadically occurs, as a
90 result of restricted vertical water exchange and bacterial decomposition of organic matter in the
91 bottom water (Hansen et al., 1999; Lennartz et al., 2014). Thus, BE is a natural laboratory to
92 study the influence of O₂ variations and anthropogenic nutrient loads on N₂O
93 production/consumption.

94 **2.2 Sample collection and measurement**

95 Monthly sampling of N₂O at the BE Time-Series Station started in July 2005. Triplicate samples
96 were collected from six depths (1, 5, 10, 15, 20 and 25 m). Seawater was drawn from 5 L Niskin
97 bottles into 20 mL brown glass vials after overflow. The vials were sealed with rubber stoppers
98 and aluminum caps. The bubble-free samples were poisoned with 50 µL of a saturated mercury
99 chloride (HgCl₂) solution and then stored in a cool, dark place until measurement. The general
100 storage time before measurements of the N₂O concentrations was less than three months.

101 The static headspace-equilibrium method was adopted to measure the dissolved N₂O
102 concentrations in the vials. 10 mL helium (99.9999 %, AirLiquide, Düsseldorf, Germany)
103 headspace was created in each vial with a gas-tight glass syringe (VICI Precision Sampling,
104 Baton Rouge, LA). Samples were vibrated with Vortex (G-560E, Scientific Industries Inc., New
105 York, USA) for 20 seconds and then left for at least two hours until equilibrium. 9.5 mL
106 subsample of the headspace was subsequently injected into a GC-ECD (gas chromatograph
107 equipped with the electron capture detector) system (Hewlett-Packard 5890 Series II, Agilent
108 Technologies, Santa Clara, CA, USA), which was calibrated with two standard gas mixtures
109 (N₂O in synthetic air, Deuste-Steininger GmbH, Mühlhausen, Germany and Westfalen AG,
110 Münster, Germany) prior to the measurement. The average precision of the measurements,



111 calculated as the median standard deviation from triplicate measurements, was 0.4 nM.
112 Triplicates with a standard deviation of >10% were omitted. More details about the N₂O
113 measurement can be found in Kock et al. (2016). Dissolved oxygen (O₂) concentrations were
114 measured by Winkler titrations (Grasshoff et al., 1999). Nutrient concentrations were measured
115 by the Segmented Continuous Flow Analysis (SCFA, Grasshoff et al., 1999). A more detailed
116 summary of the parameters measured and methods applied can be found in Lennartz et al. (2014).

117 **2.3 Times series analysis**

118 A time-series can be decomposed into three main components, i.e. trend, cycle and residual
119 component (Schlittgen and Streitberg, 2001). We used the Mann–Kendall test and wavelet
120 analysis to detect the trend and periodical cycles in the time-series data, respectively. As for the
121 residual component, we highlight unusual high/low N₂O concentrations during 2005-2017 and
122 discuss the potential causes for these events.

123 **2.3.1 Wavelet analysis**

124 In order to decipher periodical cycles of the parameters collected at the BE Time-Series Station,
125 a wavelet analysis method was adopted. Wavelet analysis enables the detection of the period and
126 the temporal occurrence of repeated cycles in time-series data. One of the requirements for
127 wavelet analysis is a regular, continuous time-series. Since there is data missing (maximum 2
128 months in a row) in the BE time-series, due to terrible weather or the ship's unavailability,
129 missing data was interpolated from the previous and following months. Data was shifted to the
130 15th of each month to obtain regular spacing. Considering the band width in both frequency and
131 time domain, a Morlet mother wavelet with a wave number of 6 was chosen (Torrence and
132 Compo, 1998). The mother wavelet was then scaled between the frequency of a half-year cycle
133 and the length of the time-series with a stepsize of 0.25. The wavelet analysis was conducted
134 with the MatLab code by Torrence and Compo [2004]. More information about the method can
135 be found on the website <http://paos.colorado.edu/research/wavelets/>.

136 **2.3.2 Mann–Kendall test**

137 Mann–Kendall test (MKT) is a non-parametric statistical test to assess the significance of
138 monotonic trends for time-series measurements. It tests the null hypothesis that all variables are
139 randomly distributed against the alternative hypothesis that a monotonic trend, either increase or
140 decrease, exists in the time-series on a given significance level α (here $\alpha=0.05$). MKT is flexible
141 for data with missing values and the results are not impacted by the magnitude of extreme values,
142 which makes it a widely used test in hydrology and climatology (e.g. Xu et al., 2003; Yang et al.,
143 2004). However, MKT is sensitive to serial correlation in the time-series. The presence of
144 positive serial correlation would increase the probability of trend detection even though no such
145 trend exists (Kulkarni and von Storch, 1995). In order to avoid this situation, data from 12
146 months were tested individually. It is assumed that there is no residual effect left from the same



147 month last year, considering that the nitrogen species are rapidly biologically cycled. The Matlab
148 function from Simone (2009) was used for the MKT.

149 **2.4 Calculation of saturation and sea-to-air flux density**

150 N₂O saturations (S_{N_2O} , %) were calculated as:

$$151 \quad S_{N_2O} = 100 \times N_{2O_{obs}}/N_{2O_{eq}} \quad (1)$$

152 where $N_{2O_{obs}}$ and $N_{2O_{eq}}$ (in nM) are the observed and equilibrated N₂O concentrations in
153 seawater, respectively. $N_{2O_{eq}}$ was computed as a function of surface seawater temperature, in
154 situ salinity (Weiss and Price, 1980) and the dry mole fractions of atmospheric N₂O at the time
155 of the sampling. The dry mole fractions of atmospheric N₂O were derived from the monthly
156 average of N₂O data measured at Mace Head, Ireland (AGAGE, <http://agage.mit.edu/>).

157 The excess of N₂O (ΔN_{2O}) and apparent oxygen utilization (AOU) was calculated as:

$$158 \quad \Delta N_{2O} = N_{2O_{obs}} - N_{2O_{eq}} \quad (2)$$

$$159 \quad AOU = O_{2eq} - O_{2obs} \quad (3)$$

160 where O_{2eq} and O_{2obs} (in μ M) are the equilibrated and observed O₂ concentrations in seawater,
161 respectively. The equilibrated O₂ concentrations were calculated with the equation given by
162 Weiss (1970).

163 N₂O flux density (F_{N_2O} , in $\text{nmol m}^{-2} \text{s}^{-1}$) was calculated as:

$$164 \quad F_{N_2O} = k_{N_2O} \times (N_{2O_{obs}} - N_{2O_{eq}}) \quad (4)$$

165 where k_{N_2O} (in cm h^{-1}) is the gas transfer velocity calculated with the method given by
166 Nightingale et al. (2000), as a function of the wind speed and the Schmidt number (Sc). The
167 wind speed data were obtained from the Kiel Lighthouse (see: www.geomar.de/service/wetter/),
168 which is approximately 20 km away from the BE Time-Series Station. The wind speed was
169 normalized to 10 m (u_{10}) to calculate k_{N_2O} (Hsu et al., 1994). k_{N_2O} was adjusted by multiplying
170 with $(Sc/600)^{-0.5}$, and Sc was computed according to Walter et al. (2004).

171 **3. Result and discussion**

172 **3.1 Overview**

173 N₂O concentrations at the BE Time-Series Station showed significant temporal and depth-
174 dependent variations from 2005 to 2017 (Fig. 2). N₂O concentrations fluctuated between 1.2 and
175 37.8 nM, with an overall average of 13.9 ± 4.2 nM. This value was higher than the results from
176 the surface water of Station ALOHA ($5.9\text{--}7.4$ nmol kg^{-1} , average 6.5 ± 0.3 nmol kg^{-1} , Wilson et
177 al., 2017), which is reasonable considering the weak anthropogenic impact in the North Pacific



178 Subtropical Gyre. The N_2O concentrations at BE were much lower than those measured at the
179 time-series station in the coastal upwelling area off Chile ($2.9\text{--}492\text{ nM}$, average $39.4\pm 29.2\text{ nM}$ in
180 the oxyclines and $37.6\pm 23.3\text{ nM}$ in the bottom waters, Farías et al., 2015) and a quasi-time series
181 station off Goa (Naqvi et al., 2010), where significant N_2O accumulations were observed in
182 subsurface waters at both locations. Our measurements were comparable to the time-series
183 station from Saanich Inlet ($\sim 0.5\text{--}37.4\text{ nM}$, average 14.7 nM , Capelle et al., 2018), a seasonally
184 anoxic fjord which has similar hydrographic conditions as BE.

185 NO_2^- concentrations fluctuated between below detection limit of $0.1\text{ }\mu\text{M}$ and $1.6\text{ }\mu\text{M}$, with an
186 average of $0.2\pm 0.3\text{ }\mu\text{M}$. NO_3^- concentrations varied from below detection limit of $0.3\text{ }\mu\text{M}$ to 17.9
187 μM , with an average of $2.0\pm 2.8\text{ }\mu\text{M}$. The temporal and spatial distributions of nitrite (NO_2^-) and
188 nitrate (NO_3^-) were similar during 2005–2017. A clear O_2 seasonality can be seen with severe O_2
189 depletion in the bottom waters during summer and autumn. Anoxia with the presence of H_2S
190 were detected in September/October 2005, September 2007, September/October 2014, and
191 September–November 2016. All of the extremely low N_2O concentrations ($<5\text{ nM}$) were
192 observed in the bottom waters in autumn, coinciding with hypoxia/anoxia, while the high N_2O
193 concentrations ($>20\text{ nM}$) sporadically occurred at different depths either in spring or autumn.

194 3.2 Seasonal cycle

195 Significant cycles at different frequencies were detected via wavelet analysis at the BE Time-
196 Series Station during 2005–2017 (Fig. 3). A half-year NO_2^- cycle sporadically occurred in 2007–
197 2009, 2013 and 2015. There is a seasonal NO_2^- variability (at the frequency of 1 year) between
198 2007 and 2016 (times before 2007 and after 2016 were outside the conic line), except during
199 2010–2012, when high NO_2^- concentrations were not observed in winter (Fig. 2). A biennial
200 cycle of NO_2^- could be observed as well during 2008–2015. The NO_3^- concentrations were
201 dominated by an annual cycle and a minor half-year cycle. The biennial cycle only occurred in
202 2008 and 2009. A remarkable seasonal variability of dissolved O_2 prevailed all the time, which is
203 also obvious from the times series data shown in Fig. 2. The annual N_2O cycle became gradually
204 more and more evident until 2014, then declined and reoccurred less intensely in 2016. The
205 periodical cycle was also present at other frequencies, indicated by the broadening of the red area
206 before 2015 in Fig. 2d. For example, a biennial N_2O cycle occurred during 2013–2015.

207 The half-year cycles of NO_2^- and NO_3^- were probably associated with algae blooms which
208 usually occur in each spring and autumn (Smetacek, 1985; Bange et al., 2010). Since the time
209 between the two blooms differed between years, the cycles were weak and thus not present in
210 every year. Due to the fact that there was no half-year O_2 cycle at all, nutrients apart from O_2
211 might be the “drivers” of the sporadic half-year N_2O cycle in 2008 and 2015, because N_2O
212 production depends on the concentration of the bioavailable nitrogen compounds (Codispoti et
213 al., 2001).



214 Generally the wavelet analysis indicated a strong annual cycle for NO_2^- , NO_3^- , dissolved O_2 and
215 N_2O at the BE Time-Series Station, which enabled us to explore the seasonal pattern with annual
216 mean data. Although extreme values were excluded as a result of averaging, the smoothed results
217 generally reflect the seasonality of these parameters. Here, we focus on the annual cycle.

218 The annual mean vertical distribution of dissolved O_2 , NO_2^- , NO_3^- and N_2O are shown in Fig. 4.
219 Due to the development of stratification, the mixed layer was shallow in summer and deep in late
220 autumn/winter. O_2 depletion was observed in bottom waters from late spring until late autumn.
221 The seasonal distributions of NO_2^- and NO_3^- were similar and significantly correlated with high
222 concentrations observed in winter ($[\text{NO}_3^-]=11.59[\text{NO}_2^-]-0.51$, $R^2=0.80$, $n=72$, $p<0.0001$).
223 Minimum N_2O concentrations were found in the bottom waters during September and October,
224 presumably as a result of consumption during denitrification under anoxic condition (Codispoti
225 et al., 2005). High N_2O concentrations were observed in late spring and late autumn, respectively.
226 In late spring N_2O accumulated in the bottom waters because the stratification prevented mixing
227 of the water column. In late autumn, however, N_2O could be ventilated to the surface and thus
228 emitted to the atmosphere due to the breakdown of the stratification. The high N_2O
229 concentrations could be attributed to enhanced N_2O production via nitrification and/or
230 denitrification within the oxic/anoxic interface (Goreau et al., 1980; Codispoti et al., 1992). Since
231 there is no clear O_2 concentration threshold, N_2O production from both nitrification and the onset
232 of denitrification overlap at oxic/anoxic interface. To this end, direct N_2O production
233 measurements (i.e. nitrification/denitrification rates) are required to decipher which process
234 dominates the formation of the different N_2O maxima.

235 High N_2O concentrations prevailed all over the water column in winter/early spring. NH_4^+
236 is released from the sediment into bottom waters due to the degradation of organic matter (Dale et
237 al., 2011), especially after the autumn algae bloom. The stratification usually completely breaks
238 down at this time of the year and the water column becomes oxygenated. Denitrification is
239 inhibited by the presence of O_2 and thus nitrification is presumably responsible for the high N_2O
240 concentrations in winter/early spring. This is supported by the positive correlation between pH
241 and N_2O concentrations in December, January and February during 2005–2017 (Fig. 5). An
242 increase in pH would shift the $\text{NH}_3:\text{NH}_4^+$ equilibrium and provide more available NH_3 for
243 nitrification. Similar relationship between pH and N_2O production also was reported in sub-polar
244 and polar Atlantic Ocean (Rees et al., 2016).

245 **3.3 Trend analysis**

246 The MKTs were conducted for the surface (1m) and bottom (25m) N_2O concentrations and
247 saturations of the individual 12 months, respectively. Significant decreasing trends were detected
248 for the concentrations in the bottom waters for February and August (Table 1a), and for the
249 saturations in the surface for September and in the bottom for August and November (Table 1b).
250 These results indicated that some systematical changes in N_2O took place at BE. For example,
251 the significant decrease in N_2O concentration/saturation in August might be associated with the



252 increasing temperature, which reinforces the stratification and accelerates O₂ consumption in the
253 bottom waters (Lennartz et al., 2014). As a result, hypoxia/anoxia starts earlier and thus enables
254 the onset of denitrification to consume N₂O. During most of the months, trends in N₂O
255 concentration and saturation were not significant during 2005–2017.

256 A significant nutrient decline has been observed at the BE Time-Series Station since the mid-
257 1980s, however, Lennartz et al. (2014) found that bottom O₂ concentrations were still decreasing
258 over the past 60 years. The ongoing oxygen decline was attributed to the temperature-enhanced
259 O₂ consumption in the bottom water (Meier et al., 2018) and a prolongation of the stratification
260 period at the BE Time-Series Station (Lennartz et al., 2014). Please note that the trends in
261 nutrients and O₂ concentrations were detected based on the data collection which lasted for
262 approximately 30 and 60 years, respectively, while the N₂O observations at BE Time-Series
263 Station has lasted for only 12.5 years. Further MKT analysis for nutrients, temperature and
264 oxygen for months with significant trends in N₂O concentrations did not show any significant
265 results ($p > 0.05$). The significant trends in N₂O concentrations thus do not seem to be directly
266 related to one of these parameters, and we cannot state a reason for the significant trends of N₂O
267 concentration in February and the N₂O saturation in September and November at this point.
268 Presumably, a longer monitoring period for N₂O is required to detect corresponding trends in
269 N₂O and oxygen or nutrients.

270 **3.4 Extreme events**

271 **3.4.1 Low N₂O concentrations during October 2016–April 2017**

272 Besides the low N₂O concentrations occurring in autumn, we observed a band of pronounced
273 low N₂O concentrations which started in October 2016 and lasted until April 2017 (Fig. 6). In
274 this period N₂O concentrations varied between 5.5–13.9 nM, with an average of 8.4 ± 2.0 nM.
275 This is approximately 40% lower than the average N₂O concentration during the entire
276 measurement period 2005–2017. The average N₂O saturation during 2005–2017 was $111 \pm 30\%$,
277 while from October 2016 to April 2017, the N₂O saturations were as low as 43–93% (average
278 $62 \pm 10\%$).

279 Undersaturated N₂O waters have been previously reported from the Baltic Sea: Rönner (1983)
280 observed a N₂O surface saturation of 79% in the central Baltic Sea and attributed the
281 undersaturation to upwelling of N₂O-depleted waters. Bange et al. (1998) found a minimum N₂O
282 saturation of 91% in the southern Baltic Sea where the hydrographic conditions were
283 significantly influenced by riverine runoff. Walter et al. (2006) reported a mean N₂O saturation
284 of $79 \pm 11\%$ for shallow stations (<30 m) in the southwestern Baltic Sea in October 2003. The
285 low-N₂O event at BE was unusual because the concentrations were much lower than those
286 reported values and it lasted for more than half a year.



287 Although the observed temperatures and salinities during October 2016–April 2017 were
288 comparable to other years, it is difficult to evaluate the role of physical mechanism in the low-
289 N₂O event because of insufficient data for water mass exchange at the BE Time-Series Station.
290 Here we mainly focused on the chemical or biological processes. Anoxia events with the
291 presence of H₂S were observed in the bottom waters for three months in a row during
292 September–November 2016. This is an unusual long period and is unprecedented at the BE
293 Time-Series Station. In December 2016 the stratification did not completely break down.
294 Although the water column was generally oxygenated, bottom O₂ concentrations were the lowest
295 observed during the past ten years. Considering the classical view of N₂O consumption via
296 denitrification under hypoxic and anoxic conditions, we inferred that denitrification accounted
297 for low N₂O concentrations in the bottom layer. However, the question still remains where the
298 low-N₂O-concentration water in the upper layers came from.

299 In September 2016, low N₂O concentrations were only observed in the bottom waters where the
300 anoxia occurred. However, the situation was different in the following months. During
301 October/November 2016, N₂O concentrations were homogeneously distributed in the water
302 column. Although the stratification gradually started to break down in late autumn, the density
303 gradient was still strong enough to keep the bottom waters at anoxic conditions and prevented
304 the low-N₂O-concentration to reach the surface. Thus we inferred that the unusual low N₂O
305 concentrations in the upper layers (above 20 m) were probably resulting from advection of
306 adjacent waters. Due to the fact that the upper layers were well-mixed and oxygenated, in situ
307 N₂O consumption in the water column could be neglected. We suggest therefore, that the N₂O
308 depleted waters were resulting from consumption of N₂O in bottom waters elsewhere and then
309 they were upwelled and transported to BE. Hence, N₂O consumption via denitrification might
310 have been, directly or indirectly, responsible for the low N₂O concentrations during October–
311 November 2016.

312 In December 2016, the bottom waters were ventilated with O₂. Although N₂O consumption by
313 denitrification should have been inhibited by the presence of O₂ (Codispoti et al., 2001), the N₂O
314 concentrations did not restore to their normal level under suboxic conditions. Since January 2017,
315 the whole water column was well mixed and oxygenated. Usually a significant nutrient supply
316 could be observed starting in November (Fig. 4) as a result of remineralization and vertical
317 mixing, but the average NO₂⁻ and NO₃⁻ concentrations during November 2016–April 2017 were
318 0.2 and 1.4 μM, respectively, which was about 50% and 60% lower than in other years.
319 Ammonium (NH₄⁺) and Chlorophyll *a* concentrations (data not shown) during this period were
320 comparable to that of other years. We did not observe an exceptional spring algae bloom in 2017,
321 indicating that assimilative uptake by phytoplankton was not responsible for the low nutrients
322 concentrations. The nutrient deficiency might be attributed to enhanced nitrogen removal
323 processes like denitrification or anammox (Voss et al., 2005; Hietanen et al., 2007; Hannig et al.,
324 2007) during the prolonged period of anoxia in autumn 2016. During the low N₂O event, we
325 found that N₂O concentrations were positively correlated with both NO₂⁻



326 $([N_2O]=7.02[NO_2^-]+7.36, R^2=0.29, n=24, p<0.01)$ and NO_3^- $([N_2O]=0.80[NO_3^-]+7.36, R^2=0.51,$
327 $n=24, p<0.0001)$. These results indicate that the development and maintenance of the low- N_2O -
328 concentration was closely associated with nutrient deficiency. Especially after the breakdown of
329 the stratification, when denitrification was no longer a significant N_2O sink, nutrients might have
330 become a limiting factor for N_2O production.

331 In general, the low- N_2O -concentration event during October 2016–April 2017 can be divided
332 into two parts: in the stratified waters during October–November 2016, O_2 played a dominant
333 role and N_2O was consumed via denitrification under anoxic conditions. In the well-mixed water
334 column during December 2016–April 2017, nutrient deficiency seemed to have constrained N_2O
335 production via nitrification under suboxic/oxic conditions.

336 In recent years a novel biological N_2O consumption pathway, called N_2O fixation, which
337 transforms N_2O into particulate organic nitrogen via its assimilation, has been reported (Farías et
338 al., 2013). This process can take place under extreme environmental conditions even at very low
339 N_2O concentrations. Cornejo et al. (2015) reported that N_2O fixation might play a major role in
340 the coastal zone off central Chile where seasonally occurring surface N_2O undersaturation was
341 observed. The relatively high N_2 fixation rates in the Baltic Sea (Sohm et al., 2011) highlight the
342 potential role of N_2O fixation (Farías et al., 2013). However, we cannot quantify the role of
343 biological N_2O fixation for the N_2O depletion in the Baltic Sea due to the absence of N_2O
344 assimilation measurements.

345 **3.4.2 High N_2O concentrations in November 2017**

346 High N_2O concentrations were observed at the BE Time-Series Station in November 2017. The
347 average value reached 35.4 ± 1.5 nM, which was the highest concentration measured during the
348 entire sampling period from 2005 to 2017. Dissolved N_2O was homogeneously distributed in the
349 water column, but this event did not last long. In December, dissolved N_2O returned to normal
350 levels and the average concentration in the water column was comparable to that of other years.
351 Average N_2O saturation in November 2017 was $322\pm 10\%$, which was also the highest for the
352 past 12.5 years. This value was much higher than the maximum surface N_2O saturation reported
353 by Rönner (1983) in the central Baltic Sea, but was comparable to the results observed in the
354 southern Baltic Sea (312%, Bange et al., 1998). Bange et al. (1998) linked the enhanced N_2O
355 concentrations to riverine runoff because those samples were collected in an estuarine area,
356 however, the riverine influence around the BE Time-Series Station is negligible. As a result, the
357 impact of fresh water input can be excluded.

358 Dissolved O_2 seemed to play a dominant role in the high N_2O concentrations. Enhanced N_2O
359 production usually occurred at the oxic/anoxic interface, which was closely linked to the
360 development of water column stratification. In general the breakdown of the stratification is
361 faster than its establishment at the BE Time-Series Station. As a result, it took about half a year
362 for bottom O_2 saturation to gradually decrease from $\sim 80\%$ to almost 0% (i.e. anoxia), but only



363 two months to restore normal saturation level in 2010 (Fig. 7). In late autumn, surface water
364 penetrated into the deep layers via vertical mixing and eroded the oxic/anoxic interface. The
365 entire water column quickly became oxygenated and the enhanced N₂O production was stopped.

366 Hypoxia/anoxia at BE is usually observed in the bottom waters in autumn, but in September
367 2017, hypoxic water (O₂ saturation < 20 %, which was close to the criterion for hypoxia, see
368 Naqvi et al., 2010) was found in the subsurface layer (10 m) as well. Surface O₂ saturation was
369 only ~50%, which was the lowest during the sampling period 2005–2017. The density gradient
370 of the water column in September 2017 was much lower than in other years. These results
371 indicate the occurrence of an upwelling event at BE Time-Series Station in autumn 2017, which
372 might be a result of the saline water inflow from the North Sea considering the change of salinity
373 in the water column. Strong vertical mixing has interrupted the hypoxia/anoxia and bottom O₂
374 saturation reached ~60% in October 2017. The presence of O₂ prevented N₂O consumption via
375 denitrification, as a result, we did not observe a significant N₂O decline during that period (Fig.
376 6).

377 Considering the fact that a significant autumn algae bloom was observed in autumn 2017 (as
378 indicated by high chlorophyll a concentrations, data not shown), severe O₂ depletion in the
379 bottom water could be expected. Although the bottom O₂ saturation was only slightly lower in
380 November than in October, we speculate that even lower O₂ saturation (but not anoxia) might
381 have occurred between October and November. The “W-shaped” O₂ saturation curve (see Fig. 7)
382 suggests that the stratification did not completely break down in October and that there might
383 have been a reestablishment of the oxic/anoxic interface providing favorable conditions for
384 enhanced N₂O production. Due to the degradation of organic nitrogen, NH₄⁺ is released from the
385 sediment into bottom waters (Dale et al., 2011), especially in autumn when O₂ is low. NH₄⁺
386 concentrations in November 2017 were lower than in other years, and NO₂⁻ concentrations were
387 higher, indicating that nitrification occurred in bottom waters. To this end, we suggest that the
388 reestablishment of the oxic/anoxic interface promoted ammonium oxidation (the first step of
389 nitrification). In this case, N₂O could have temporarily accumulated because its consumption via
390 denitrification was blocked. Meanwhile, the relatively low density gradient (i.e. low stratification)
391 allowed upward mixing of the excess N₂O to the surface. However, we inferred that that this
392 phenomenon would only last for a few days due to the rapid breakdown of stratification at the
393 BE Time-Series Station.

394 Due to the development of the pronounced stratification, the oxic/anoxic interface prevailed in
395 summer/early autumn as well, but we did not observe N₂O accumulation during these months.
396 One of the potential explanations is that enhanced N₂O production only took place within
397 particular depths where strong O₂ gradient existed, but our vertical sampling resolution was too
398 low to capture this event. Also enhanced N₂O production might be covered by the weak mixing
399 which brought low-N₂O water from the bottom to the surface.



400 The upwelling event played different roles in autumn 2016 and 2017. First, upwelling took place
401 somewhere else but at BE because of the strong density and O₂ gradient in the water column
402 during autumn 2016. Second, bottom water remained anoxic in autumn 2016, while the
403 compensated water for upwelling in 2017 penetrated through stratification and brought O₂ into
404 bottom water (Fig. 7), which caused enhanced N₂O production. Similarly, autumn upwelling was
405 detected in 2011 and 2012 when we found relatively low O₂ concentrations in subsurface layers
406 (10 m) (Fig. 2), but we did not observe an increase in bottom O₂ concentrations and N₂O
407 concentrations remained low during that time. These upwelling events seem to be driven by
408 saline water inflow considering the prominent increase in salinity, but the mechanism dominates
409 O₂ input into bottom water before the stratification break down remains unclear.

410 3.5 Flux density

411 During 2005–2017, surface N₂O saturations at the BE Time-Series Station varied from 56 % to
412 314 % (69–194 % excluding the extreme values discussed in Sect. 3.4), with an average of
413 111±30 % (111±20 % without the extreme values). Generally the water column at BE was
414 slightly oversaturated with N₂O. Our results are in good agreement with the estimated mean
415 surface N₂O saturation for the European shelf (113%, Bange, 2006).

416 We found a weak seasonal cycle for surface N₂O concentrations, with high N₂O concentrations
417 occurring in winter/early spring and low concentrations occurring in summer/autumn (Fig. 4; Fig.
418 8a, b). No pronounced seasonality was found for N₂O saturation. The trend in concentration but
419 not in saturation likely results from the modulating effect of temperature on N₂O emissions:
420 During wintertime when temperatures are low, the solubility of N₂O increases, which lowers
421 emissions and increases the N₂O concentration in the surface water. The calculation of N₂O
422 saturation takes this temperature effect into account and, hence, does not show any pronounced
423 seasonality. We thus conclude that temperature plays an important modulating role for N₂O
424 emissions.

425 The wind speed (u_{10}) at the BE Time-Series Station ranged from 1.1 to 14.0 m s⁻¹, with an
426 average of 7.0±2.7 m s⁻¹. N₂O flux densities varied from -19.0 to 105.7 μmol m⁻² d⁻¹ (-14.1–30.3
427 μmol m⁻² d⁻¹ without the extreme values), with an average of 3.5±12.4 μmol m⁻² d⁻¹ (3.3±6.5
428 μmol m⁻² d⁻¹ without the extreme values). However, the true emissions might have been
429 underestimated because our monthly sampling resolution is insufficient to capture short-term
430 N₂O accumulation events due to the fast breakdown of stratification in autumn. Our flux
431 densities are comparable to those reported by Bange et al. (1998, 0.4–7.1 μmol m⁻² d⁻¹) from the
432 coastal waters of the southern Baltic Sea, but are slightly lower than the average N₂O flux
433 density reported by Rönner (1983, 8.9 μmol m⁻² d⁻¹) from the central Baltic Sea. Please note that
434 the results of Rönner (1983) were obtained only from the summer season and therefore are
435 probably biased because of missing seasonality.



436 In December 2014, a strong saline water inflow from the North Sea was observed, which was the
437 third strongest ever recorded (Mohrholz et al., 2015). Although the salinity in December 2014
438 was comparable to other years, a remarkable increase in salinity was observed in the following
439 several months. However, we did not detect a significant N₂O anomaly or enhanced emission
440 during that time. Similarly, Walter et al. (2006) investigated the impact of the North Sea water
441 inflow on N₂O production in the southern and central Baltic Sea in 2003. The oxygenated water
442 ventilated the deep Baltic Sea and shifted anoxic to oxic condition which led to enhanced N₂O
443 production, but the accumulated N₂O was unlikely to reach the surface due to the presence of a
444 permanent halocline (Walter et al., 2006).

445 Although we observed extremely high N₂O flux density in November 2017, the low-N₂O-
446 concentration (<10 nM) events have become more and more frequent during the past ten years
447 (Fig. 2). This phenomenon seldom occurred before 2011, but remarkable low N₂O
448 concentrations can be seen in 2011 and 2013, and to a less extent in 2012 and 2014. Similar
449 events lasted for several months in 2015 and for even more than half a year during 2016–2017.
450 The most striking was that the low-N₂O-concentration water was not only detected in bottom
451 waters, but also at surface which would significantly impact the air-sea N₂O flux densities.
452 Although the MKT result did not give a significant trend for the N₂O flux densities, the data
453 presented in Fig. 9 suggest a potential decline of N₂O flux densities from the coastal Baltic Sea,
454 challenging the conventional view that N₂O emissions from coastal waters would most probably
455 increase in the future, which was based on the hypothesis of increasing nutrient loads into coastal
456 waters. Due to an effective reduction of nutrient inputs, the severe eutrophication condition in the
457 Baltic Sea has been alleviated (HELCOM, 2018b), but ongoing deoxygenation points to the fact
458 that it will take a longer time for coastal ecosystems to feedback to reduced nutrient inputs
459 because other environmental changes such as warming may override decreasing eutrophication
460 (Lennartz et al., 2014).

461 **4. Conclusions**

462 The seasonal and inter-annual N₂O variations at the BE Time-Series Station from July 2015 to
463 December 2017 were driven by the prevailing O₂ regime and nutrients availability. We found a
464 pronounced seasonal cycle with low N₂O concentrations (undersaturations) occurring in
465 hypoxic/anoxic bottom waters in autumn and enhanced concentrations (supersaturations) all over
466 the water column in winter/early spring. Significant decreasing trends for N₂O concentrations
467 were found for few months, while most of the year, no significant trend was detectable in the
468 period of 2005–2017. During 2005–2017, no significant trends were present for O₂ and nutrients
469 either, but these parameters all show significant decreasing trends on longer time scales (~60
470 years) at BE. Our results show the strong coupling of N₂O with O₂ and nutrient concentrations,
471 and suggest similar changes on comparable time scales. Further monitoring of N₂O at BE time
472 series station is thus important to detect changes. Further studies on N₂O
473 production/consumption by nitrification and denitrification and analysis of the characteristic N₂O



474 isotope signature might be very helpful to decipher the potential roles of O₂/nutrients for N₂O
475 cycling.

476 Temperature plays a modulating role for the N₂O emission at the BE Time-Series Station.
477 Although the hydrographic condition at BE is generally dominated by the inflow of saline North
478 Sea water, this did not affect N₂O production and its emissions to the atmosphere. It seems that
479 events with extremely low N₂O concentrations and thus reduced N₂O emissions became more
480 frequent in recent years. Our results provide a new perspective onto potential future patterns of
481 N₂O distribution and emissions in coastal areas. Continuous measurement at the BE Time-Series
482 Station with a focus on late autumn would be of great importance for monitoring and
483 understanding the future changes of N₂O concentrations and emissions in the southwestern Baltic
484 Sea.

485 **Author contribution**

486 X.M., S.T.L. and H.W.B. designed the study and participated in the fieldwork. N₂O
487 measurements and data processing were done by X.M. and S.T.L. X.M. wrote the manuscript
488 with contributions from S.T.L. and H.W.B.

489 **Acknowledgments**

490 The authors thank the captain and crew of the RV *Littorina* and *Polarfuchs* as well as the many
491 colleagues and numerous students who helped with the sampling and measurements of the BE
492 time-series through various projects. Special thanks to A. Kock for her help with sampling,
493 measurements and data analysis. The time-series at BE was supported by DWK
494 Meeresforschung (1957–1975), HELCOM (1979–1995), BMBF (1995–1999), the Institut für
495 Meereskunde (1999–2003), IfM-GEOMAR (2004–2011) and GEOMAR (2012–present). The
496 current N₂O measurements at BE are supported by the EU BONUS INTEGRAL project which
497 receives funding from BONUS (Art 185), funded jointly by the EU, the German Federal
498 Ministry of Education and Research, the Swedish Research Council Formas, the Academy of
499 Finland, the Polish National Centre for Research and Development, and the Estonian Research
500 Council. The Boknis Eck Time-Series Station (www.bokniseck.de) is run by the Chemical
501 Oceanography Research Unit of GEOMAR, Helmholtz Centre for Ocean Research Kiel. Data
502 from BE are available from www.bokniseck.de/database-access. The N₂O data presented here
503 have been archived in MEMENTO (the MarinE MethanE and NiTrous Oxide database:
504 <https://memento.geomar.de>). X. Ma is grateful to the China Scholarship Council for providing
505 financial support (File No. 201306330056) and the EU BONUS INTEGRAL project.

506 **References**

507 Bange, H. W.: Nitrous oxide and methane in European coastal waters, *Estuar. Coast. Shelf S.*, 70,
508 361–374, <https://doi.org/10.1016/j.ecss.2006.05.042>, 2006.



- 509 Bange, H. W., Dahlke, S., Ramesh, R., Meyer-Reil, L. A., Rapsomanikis, S., and Andreae, M. O.:
510 Seasonal study of methane and nitrous oxide in the coastal waters of the southern Baltic Sea,
511 *Estuar. Coast. Shelf S.*, 47, 807–817, <https://doi.org/10.1006/ecss.1998.0397>, 1998.
- 512 Bange, H. W., Bergmann, K., Hansen, H. P., Kock, A., Koppe, R., Malien, F., and Ostrau, C.:
513 Dissolved methane during hypoxic events at the Boknis Eck Time Series Station (Eckernförde
514 Bay, SW Baltic Sea), *Biogeosciences*, 7, 1279–1284, <https://doi.org/10.5194/bg-7-1279-2010>,
515 2010.
- 516 Battaglia, G. and Joos, F.: Marine N₂O emissions from nitrification and denitrification
517 constrained by modern observations and projected in multimillennial global warming simulations,
518 *Global Biogeochem. Cy.*, 32, 92–121, <https://doi.org/10.1002/2017GB005671>, 2018.
- 519 Bonin, P., Gilewicz, M., and Bertrand, J. C.: Effects of oxygen on each step of denitrification on
520 *Pseudomonas nautica*, *Can. J. Microbiol.*, 35, 1061–1064, <https://doi.org/10.1139/m89-177>, 1989.
- 521 Breitburg, D., Levin, L. A., Oschlies, A., Grégoire, M., Chavez, F. P., Conley, D. J., Garçon, V.,
522 Gilbert, D., Gutiérrez, D., Isensee, K., Jacinto, G. S., Limburg, K. E., Montes, I., Naqvi, S. W. A.,
523 Pitcher, G. C., Rabalais, N. N., Roman, M. R., Rose, K. A., Seibel, B. A., Telszewski, M.,
524 Yasuhara, M., and Zhang, J.: Declining oxygen in the global ocean and coastal waters, *Science*,
525 359, eaam7240, <http://dx.doi.org/10.1126/science.aam7240>, 2018.
- 526 Capelle, D. W., Hawley, A. K., Hallam, S. J., and Tortell, P. D.: A multi-year time-series of N₂O
527 dynamics in a seasonally anoxic fjord: Saanich Inlet, British Columbia, *Limnol. Oceanogr.*, 63,
528 524–539, <https://doi.org/10.1002/lno.10645>, 2018.
- 529 Carstensen, J., Andersen, J. H., Gustafsson, B. G., and Conley, D. J.: Deoxygenation of the
530 Baltic Sea during the last century, *P. Natl. Acad. Sci. USA*, 111, 5628–5633,
531 <https://doi.org/10.1073/pnas.1323156111>, 2014.
- 532 Codispoti, L. A., Elkins, J. W., Yoshinari, T., Fredrich, G., Sakamoto, C., and Packard, T.: On
533 the nitrous oxide flux from productive regions that contain low oxygen waters, in: *Oceanography*
534 *of the Indian Ocean*, edited by Desai, B. N., Oxford Univ. Press, New York, 271–284, 1992.
- 535 Codispoti, L. A., Brandes, J. A., Christensen, J. P., Devol, A. H., Naqvi, S. W. A., Paerl, H. W.,
536 and Yoshinari, T.: The oceanic fixed nitrogen and nitrous oxide budgets: Moving targets as we
537 enter the anthropocene? *Sci. Mar.*, 65, 85–105, <https://doi.org/10.3989/scimar.2001.65s285>, 2001.
- 538 Codispoti, L. A., Yoshinari, T., and Devol, A. H.: Suboxic respiration in the oceanic water
539 column, in: *Respiration in aquatic ecosystems*, edited by del Giorgio, P. A. and Williams, P. J.,
540 Oxford Univ. Press, New York, 225–247, 2005.



- 541 Conley, D. J., Carstensen, J., Aigars, J., Axe, P., Bonsdorff, E., Eremina, T., and Lannegren, C.:
542 Hypoxia is increasing in the coastal zone of the Baltic Sea, *Environ. Sci. Technol.*, 45, 6777–
543 6783, doi: 10.1021/es201212r, 2011.
- 544 Cornejo, M., Murillo, A. A., and Farías, L.: An unaccounted for N₂O sink in the surface water of
545 the eastern subtropical South Pacific: Physical versus biological mechanisms, *Prog. Oceanogr.*,
546 137, 12–23, <https://doi.org/10.1016/j.pocean.2014.12.016>, 2015.
- 547 Dale, A. W., Sommer, S., Bohlen, L., Treude, T., Bertics, V. J., Bange, H. W., Pfannkuche, O.,
548 Schorp, T., Mattsdotter, M., and Wallmann, K.: Rates and regulation of nitrogen cycling in
549 seasonally hypoxic sediments during winter (Boknis Eck, SW Baltic Sea): Sensitivity to
550 environmental variables, *Estuar. Coast. Shelf S.*, 95, 14–28,
551 <https://doi.org/10.1016/j.ecss.2011.05.016>, 2011.
- 552 Ducklow, H. W., Doney, S. C., and Steinberg, D. K.: Contributions of long-term research and
553 time-series observations to marine ecology and biogeochemistry, *Annu. Rev. Mar. Sci.*, 1, 279–
554 302, <https://doi.org/10.1146/annurev.marine.010908.163801>, 2009.
- 555 Farías, L., Castro-González, M., Cornejo, M., Charpentier, J., Faúndez, J., Boontanon, N., and
556 Yoshida, N.: Denitrification and nitrous oxide cycling within the upper oxycline of the eastern
557 tropical South Pacific oxygen minimum zone, *Limnol. Oceanogr.*, 54, 132–144,
558 <https://doi.org/10.4319/lo.2009.54.1.0132>, 2009.
- 559 Farías, L., Faúndez, J., Fernández, C., Cornejo, M., Sanhueza, S., and Carrasco, C.: Biological
560 N₂O fixation in the Eastern South Pacific Ocean and marine cyanobacterial cultures, *Plos one*, 8,
561 e63956, <https://doi.org/10.1371/journal.pone.0063956>, 2013.
- 562 Farías, L., Besoain, V., and García-Loyola, S.: Presence of nitrous oxide hotspots in the coastal
563 upwelling area off central Chile: an analysis of temporal variability based on ten years of a
564 biogeochemical time series, *Environ. Res. Lett.*, 10, 044017, doi:10.1088/1748-
565 9326/10/4/044017, 2015.
- 566 Goreau, T. J., Kaplan, W. A., Wofsy, S. C., McElroy, M. B., Valois, F. W., and Watson, S.W.:
567 Production of NO₂⁻ and N₂O by nitrifying bacteria at reduced concentrations of oxygen, *Appl.*
568 *Environ. Microb.*, 40, 526–532, 1980.
- 569 Grasshoff, K., Kremling, K., and Ehrhardt, M.: *Methods of seawater analysis*, 3rd edition,
570 WILEY-VCH, Weinheim, Germany, 1999.
- 571 Hannig, M., Lavik, G., Kuypers, M. M. M., Woebken, D., Martens-Habbena, W., and Jürgens,
572 K.: Shift from denitrification to anammox after inflow events in the central Baltic Sea, *Limnol.*
573 *Oceanogr.*, 52, 1336–1345, 2007.



- 574 Hansen, H. P., Giesenhausen, H. C., and Behrends, G.: Seasonal and long-term control of bottom
575 water oxygen deficiency in a stratified shallow-coastal system, *ICES J. Mar. Sci.*, 56, 65–71, doi:
576 10.1006/jmsc.1999.0629, 1999.
- 577 HELCOM: Sources and pathways of nutrients to the Baltic Sea, *Baltic Sea Environ. Proc.*, 153,
578 2018a.
- 579 HELCOM: State of the Baltic Sea - Second HELCOM holistic assessment 2011–2016, *Baltic*
580 *Sea Environ. Proc.*, 155, <http://stateofthebalticsea.helcom.fi/>, 2018b.
- 581 Hietanen, S., and Lukkari, K.: Effects of short-term anoxia on benthic denitrification, nutrient
582 fluxes and phosphorus forms in coastal Baltic sediment, *Aquat. Microb. Ecol.*, 49, 293–302,
583 <https://doi.org/10.3354/ame01146>, 2007.
- 584 Hsu, S. A., Meindl, E. A., and Gilhousen, D. B.: Determining the power-law wind-profile
585 exponent under near-neutral stability conditions at sea, *J. Appl. Meteorol.*, 33, 757–765,
586 [https://doi.org/10.1175/1520-0450\(1994\)033<0757:DTPLWP>2.0.CO;2](https://doi.org/10.1175/1520-0450(1994)033<0757:DTPLWP>2.0.CO;2), 1994.
- 587 IPCC: Climate Change 2013: The physical science basis. Contribution of Working Group I to the
588 fifth assessment report of the Intergovernmental Panel on Climate Change, Cambridge
589 University Press, Cambridge, UK and New York, NY, 2013.
- 590 Landolfi, A., Somes, C. J., Koeve, W., Zamora, L. M., and Oschlies, A.: Oceanic nitrogen
591 cycling and N₂O flux perturbations in the Anthropocene, *Global Biogeochem. Cy.*, 31, 1236–
592 1255, doi:10.1002/2017GB005633, 2017.
- 593 Lennartz, S. T., Lehmann, A., Herrford, J., Malien, F., Hansen, H. P., Biester, H., and Bange, H.
594 W.: Long-term trends at the Boknis Eck time series station (Baltic Sea), 1957–2013: does
595 climate change counteract the decline in eutrophication? *Biogeosciences*, 11, 6323–6339,
596 <https://doi.org/10.5194/bg-11-6323-2014>, 2014.
- 597 Löscher, C. R., Kock, A., Könneke, M., LaRoche, J., Bange, H. W., and Schmitz, R. A.:
598 Production of oceanic nitrous oxide by ammonia-oxidizing archaea, *Biogeosciences*. 9, 2419–
599 2429, <https://doi.org/10.5194/bg-9-2419-2012>, 2012.
- 600 Kock, A., Arévalo-Martínez, D. L., Löscher, C. R., and Bange, H. W.: Extreme N₂O
601 accumulation in the coastal oxygen minimum zone off Peru, *Biogeosciences*. 13, 827–840, doi:
602 10.5194/bg-13-827-2016, 2016.
- 603 Kroeze, C., and Seitzinger, S. P.: Nitrogen inputs to rivers, estuaries and continental shelves and
604 related nitrous oxide emissions in 1990 and 2050: a global model, *Nutr. Cycl. Agroecosys.*, 52,
605 195–212, 1998.
- 606 Kulkarni, A., and Von Storch, H.: Monte Carlo experiments on the effect of serial correlation on
607 the Mann-Kendall test of trend, *Meteorol. Z.*, 4, 82–85, 1995.



- 608 Martinez-Rey, J., Bopp, L., Gehlen, M., Tagliabue, A., and Gruber, N.: Projections of oceanic
609 N₂O emissions in the 21st century using the IPSL Earth system model, *Biogeosciences*, 12,
610 4133–4148, doi: 10.5194/bg-12-4133-2015, 2015.
- 611 Meier, H. M., Väli, G., Naumann, M., Eilola, K., and Frauen, C.: Recently accelerated oxygen
612 consumption rates amplify deoxygenation in the Baltic Sea, *J. Geophys. Res.-Oceans.*, 123,
613 3227–3240, <https://doi.org/10.1029/2017JC013686>, 2018.
- 614 Mohrholz, V., Naumann, M., Nausch, G., Krüger, S., and Gräwe, U.: Fresh oxygen for the Baltic
615 Sea-An exceptional saline inflow after a decade of stagnation, *J. Marine Syst.*, 148, 152–166,
616 <https://doi.org/10.1016/j.jmarsys.2015.03.005>, 2015.
- 617 Naqvi, S. W. A., Jayakumar, D. A., Narvekar, P. V., Naik, H., Sarma, V. V. S. S., D'souza, W.,
618 Joseph, S., and George, M. D.: Increased marine production of N₂O due to intensifying anoxia
619 on the Indian continental shelf, *Nature*, 408, 346, 2000.
- 620 Naqvi, S.W.A., Bange, H.W., Fariás, L., Monteiro, P.M.S., Scranton, M.I., and Zhang, J.: Marine
621 hypoxia/anoxia as a source of CH₄ and N₂O, *Biogeosciences*, 7, 2159–2190,
622 <https://doi.org/10.5194/bg-7-2159-2010>, 2010.
- 623 Nevison, C., Butler, J. H., and Elkins, J. W.: Global distribution of N₂O and the ΔN₂O-AOU
624 yield in the subsurface ocean, *Global Biogeochem. Cy.*, 17,
625 <https://doi.org/10.1029/2003GB002068>, 2003.
- 626 Nightingale, P., G. Malin, C. S. Law, A. J. Watson, P. S. Liss, M. I. Liddicoat, J. Boutin, and R.
627 C. Upstill-Goddard: In situ evaluation of air-sea gas exchange parameterizations using novel
628 conservative and volatile tracers, *Global Biogeochem. Cy.*, 14, 373–387,
629 <https://doi.org/10.1029/1999GB900091>, 2000.
- 630 Rabalais, N. N., Cai, W.-J., Carstensen, J., Conley, D. J., Fry, B., Hu, X., Quinones-Rivera, Z.,
631 Rosenberg, R., Slomp, C. P., Turner, R. E., Voss, M., Wissel, B., and Zhang, J.: Eutrophication-
632 driven deoxygenation in the coastal ocean, *Oceanography*, 27, 172–183,
633 <https://doi.org/10.5670/oceanog.2014.21>, 2014.
- 634 Ravishankara, A. R., Danielm J., S., and Portmann, R. W.: Nitrous oxide (N₂O): the dominant
635 ozone-depleting substance emitted in the 21st century, *Science*, 326, 123–125, doi:
636 10.1126/science.1176985, 2009.
- 637 Rees, A. P., Brown, I. J., Jayakumar, A., and Ward, B. B.: The inhibition of N₂O production by
638 ocean acidification in cold temperate and polar waters, *Deep-Sea Res. Pt. II*, 127, 93–101,
639 <https://doi.org/10.1016/j.dsr2.2015.12.006>, 2016.



- 640 Rönner, U.: Distribution, production and consumption of nitrous oxide in the Baltic Sea,
641 Geochim. Cosmochim. Ac., 47, 2179–2188, [https://doi.org/10.1016/0016-7037\(83\)90041-8](https://doi.org/10.1016/0016-7037(83)90041-8),
642 1983.
- 643 Schlittgen, R., and Streitberg, B. H. J.: Zeitreihenanalyse, Oldenburg Wissenschaftsverlag,
644 Munich, Germany, 2001.
- 645 Seitzinger, S. P., and Kroeze, C.: Global distribution of nitrous oxide production and N inputs in
646 freshwater and coastal marine ecosystems, Global Biogeochem. Cy., 12, 93–113, 1998.
- 647 Simone, F.: Mann-Kendall Test, MathWorks,
648 <https://ww2.mathworks.cn/matlabcentral/fileexchange/25531-mann-kendall-test>, 2009.
- 649 Smetacek, V.: The annual cycle of Kiel Bight plankton: A long-term analysis, Estuaries, 8, 145–
650 157, 1985.
- 651 Sohm, J. A., Webb, E. A., and Capone, D. G.: Emerging patterns of marine nitrogen fixation, Nat.
652 Rev. Microbiol., 9, 499–508, doi: 10.1038/nrmicro2594, 2011.
- 653 Torrence, C., and Compo, G. P.: A practical guide to wavelet analysis, B. Am. Meteorol. Soc.,
654 79, 61–78, [https://doi.org/10.1175/1520-0477\(1998\)079<0061:APGTWA>2.0.CO;2](https://doi.org/10.1175/1520-0477(1998)079<0061:APGTWA>2.0.CO;2), 1998.
- 655 Torrence, C., and Compo, G. P.: Wavelet analysis, <http://paos.colorado.edu/research/wavelets/>,
656 2004.
- 657 Voss, M., Emeis, K. C., Hille, S., Neumann, T., and Dippner, J. W.: Nitrogen cycle of the Baltic
658 Sea from an isotopic perspective, Global Biogeochem. Cy., 19, doi: 10.1029/2004GB002338,
659 2005.
- 660 Walter, S., Bange, H. W., and Wallace, D. W. R.: Nitrous oxide in the surface layer of the
661 tropical North Atlantic Ocean along a west to east transect, Geophys. Res. Lett., 31, L23S07,
662 <https://doi.org/10.1029/2004GL019937>, 2004.
- 663 Walter, S., Breitenbach, U., Bange, H. W., Nausch, G., and Wallace, D. W.: Distribution of N₂O
664 in the Baltic Sea during transition from anoxic to oxic conditions, Biogeosciences, 3, 557–570,
665 <https://doi.org/10.5194/bg-3-557-2006>, 2006.
- 666 Weiss, R. F.: The solubility of nitrogen, oxygen and argon in water and seawater, Deep-Sea Res.,
667 17, 721–735, [https://doi.org/10.1016/0011-7471\(70\)90037-9](https://doi.org/10.1016/0011-7471(70)90037-9), 1970.
- 668 Weiss, R. F., and Price, B. A.: Nitrous oxide solubility in water and seawater, Mar. Chem., 8,
669 347–359, [https://doi.org/10.1016/0304-4203\(80\)90024-9](https://doi.org/10.1016/0304-4203(80)90024-9), 1980.



- 670 Wilson, S. T., Ferrón, S., and Karl, D. M.: Interannual variability of methane and nitrous oxide in
671 the North Pacific Subtropical Gyre, *Geophys. Res. Lett.*, 44, 9885–9892,
672 <https://doi.org/10.1002/2017GL074458>, 2017.
- 673 Xu, Z. X., Takeuchi, K., and Ishidaira, H.: Monotonic trend and step changes in Japanese
674 precipitation, *J. Hydrol.*, 279, 144–150, [https://doi.org/10.1016/S0022-1694\(03\)00178-1](https://doi.org/10.1016/S0022-1694(03)00178-1), 2003.
- 675 Yang, D., Li, C., Hu, H., Lei, Z., Yang, S., Kusuda, T., Koike, T., and Musiaka, K.: Analysis of
676 water resources variability in the Yellow river of China during the last half century using the
677 historical data, *Water Resour. Res.*, 40, 1–12, <https://doi.org/10.1029/2003WR002763>, 2004.
- 678 Zhang, G.-L., Zhang, J., Liu, S.-M., Ren, J.-L., and Zhao, Y.-C.: Nitrous oxide in the Changjiang
679 (Yangtze River) estuary and its adjacent marine area: Riverine input, sediment release and
680 atmospheric fluxes, *Biogeosciences*, 7, 3505–3516, <https://doi.org/10.5194/bg-7-3505-2010>,
681 2010.



682 Table 1. The results of the Mann-Kendall test for the surface and bottom N₂O concentrations and
 683 saturations of the 12 individual months.

684 Table 1a. MKT results for N₂O concentrations

Month	January		February		March		April	
Depth/m	1	25	1	25	1	25	1	25
p	0.09	0.19	0.11	0.03(-)	0.19	0.63	0.09	0.30
Month	May		June		July		August	
Depth/m	1	25	1	25	1	25	1	25
p	0.63	0.24	0.15	0.95	0.16	0.16	0.20	0.03(-)
Month	September		October		November		December	
Depth/m	1	25	1	25	1	25	1	25
p	0.25	0.76	0.36	0.76	0.67	0.16	0.10	0.30

685

686

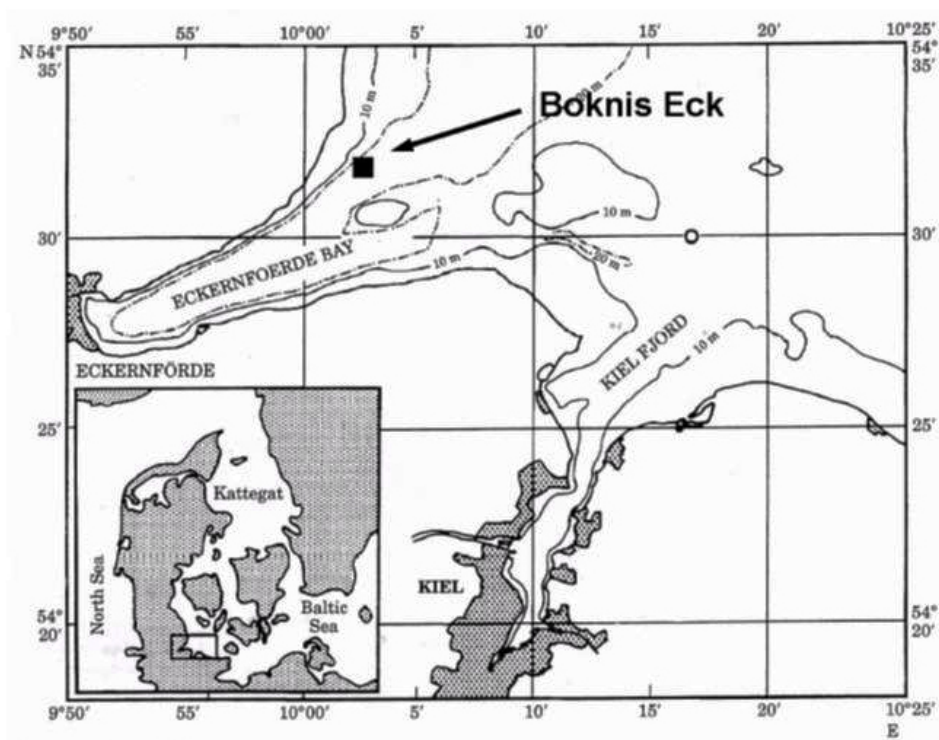
Table 1b. MKT results for N₂O saturations

Month	January		February		March		April	
Depth/m	1	25	1	25	1	25	1	25
p	0.37	0.24	0.15	0.15	0.19	0.63	0.11	0.19
Month	May		June		July		August	
Depth/m	1	25	1	25	1	25	1	25
p	0.19	1	0.37	0.54	0.10	0.43	0.20	0.02(-)
Month	September		October		November		December	
Depth/m	1	25	1	25	1	25	1	25
p	0.04(-)	0.85	0.06	0.43	0.20	0.03(-)	0.16	0.36

687

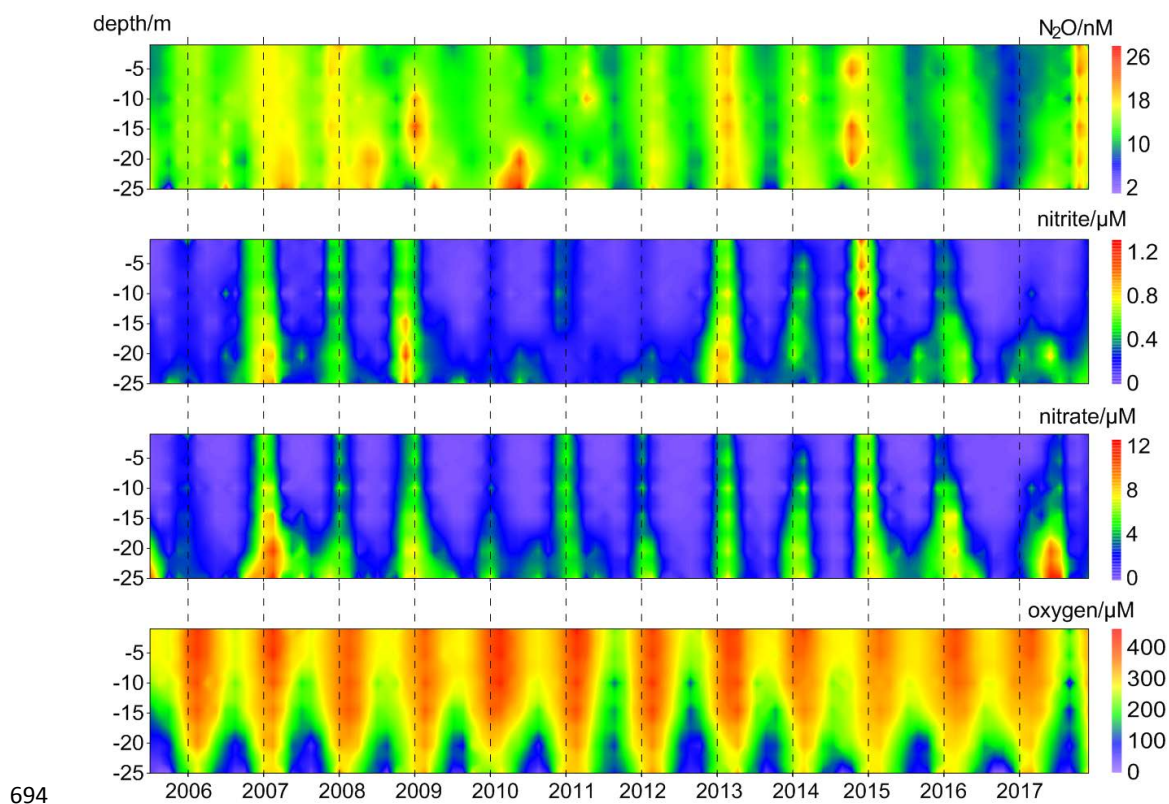
688 p indicates the p-value of the test, which is the probability, under the null hypothesis, of obtaining a value of
 689 the test statistic as extreme or more extreme than the value computed from the sample.

690 (-) indicates a rejection of the null hypothesis at α significance level and a decreasing trend is detected.



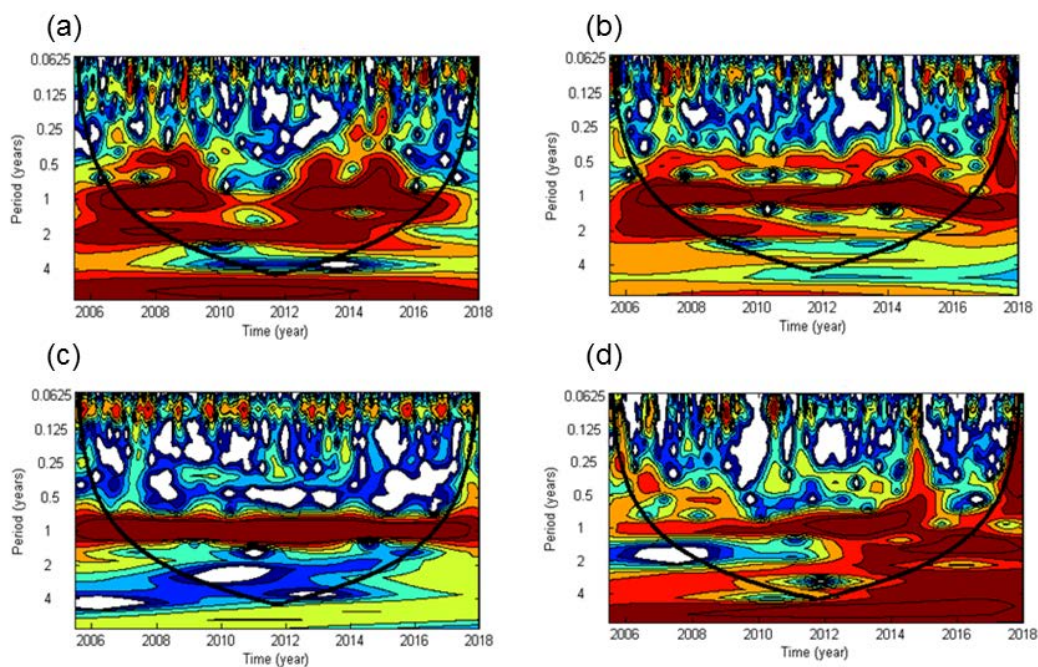
691

692 Fig. 1 Location of the Boknis Eck Time-Series Station in the Eckernförde Bay, southwestern Baltic Sea. (Map
693 from Hansen et al., 1999)



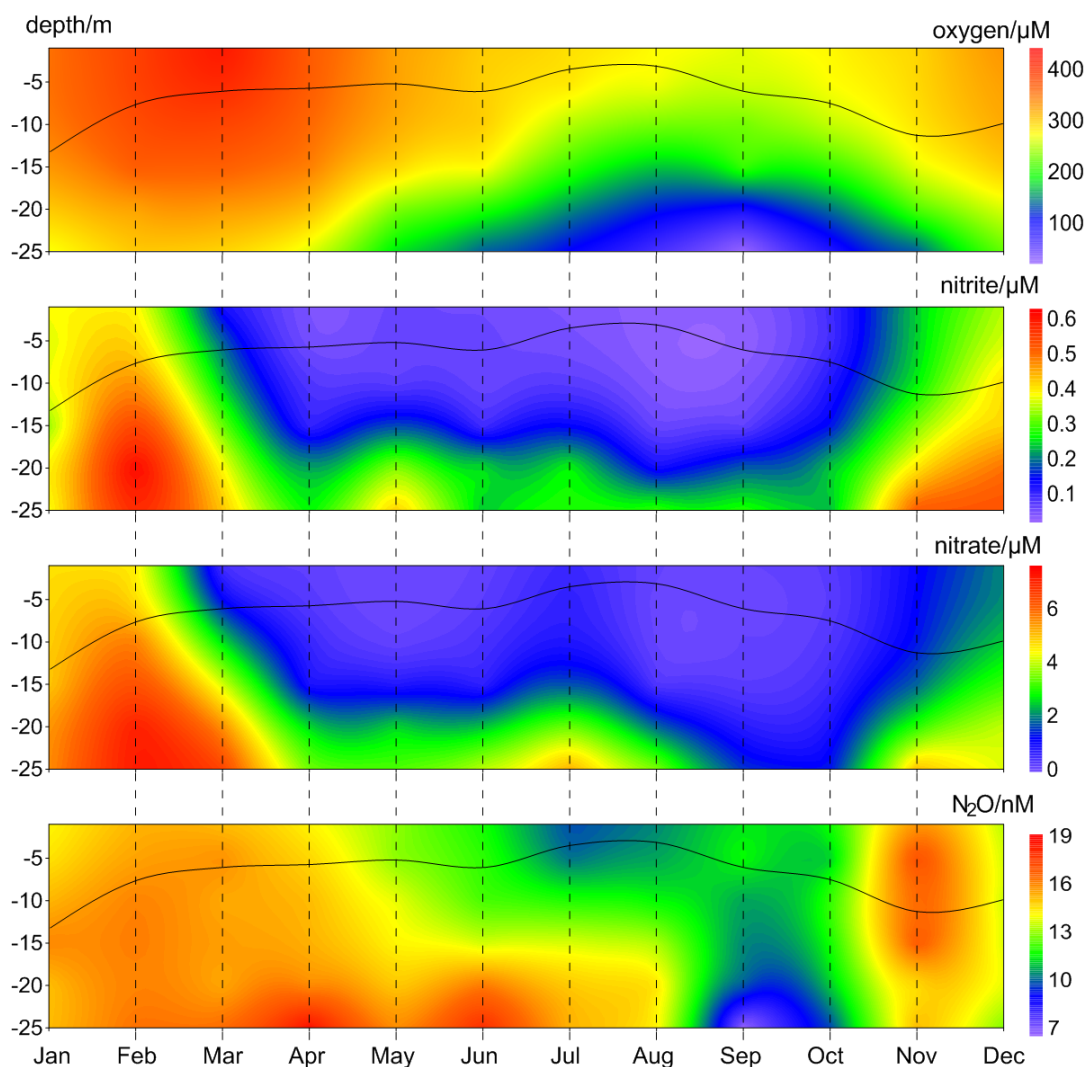
694

695 Fig. 2 Vertical distributions of dissolved O_2 , NO_2^- , NO_3^- , and N_2O from the BE Time-Series Station during
696 2005–2017.



697

698 Fig. 3 Wavelet power spectra of NO_2^- (a), NO_3^- (b), dissolved O_2 (c) and N_2O (d) from the BE Time-Series
699 Station. Red areas indicate high, blue indicate low power. The black conic line indicates the significant area
700 where boundary effects can be excluded.



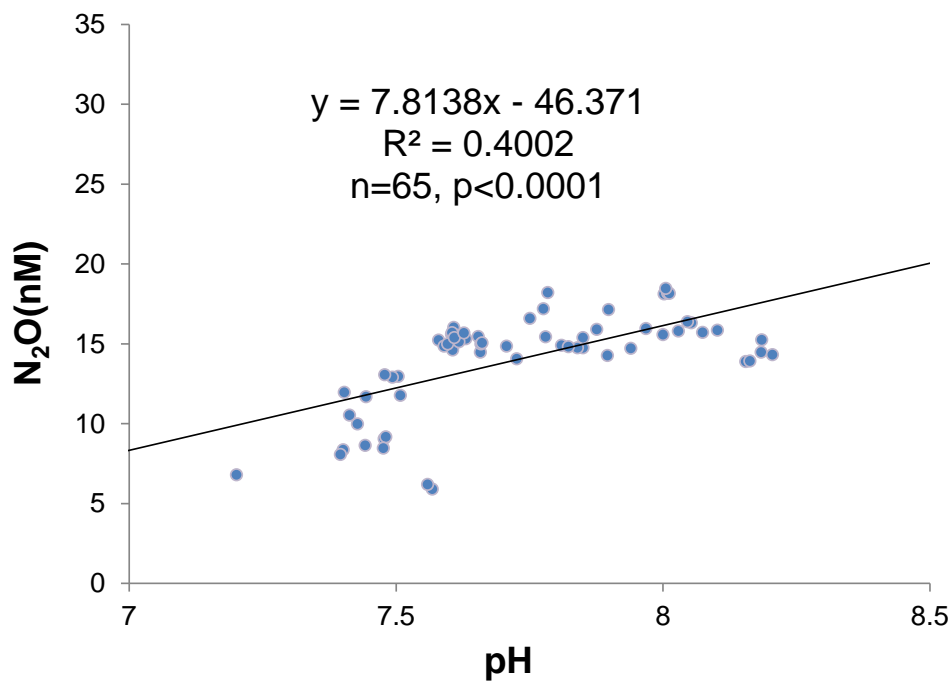
701

702

703

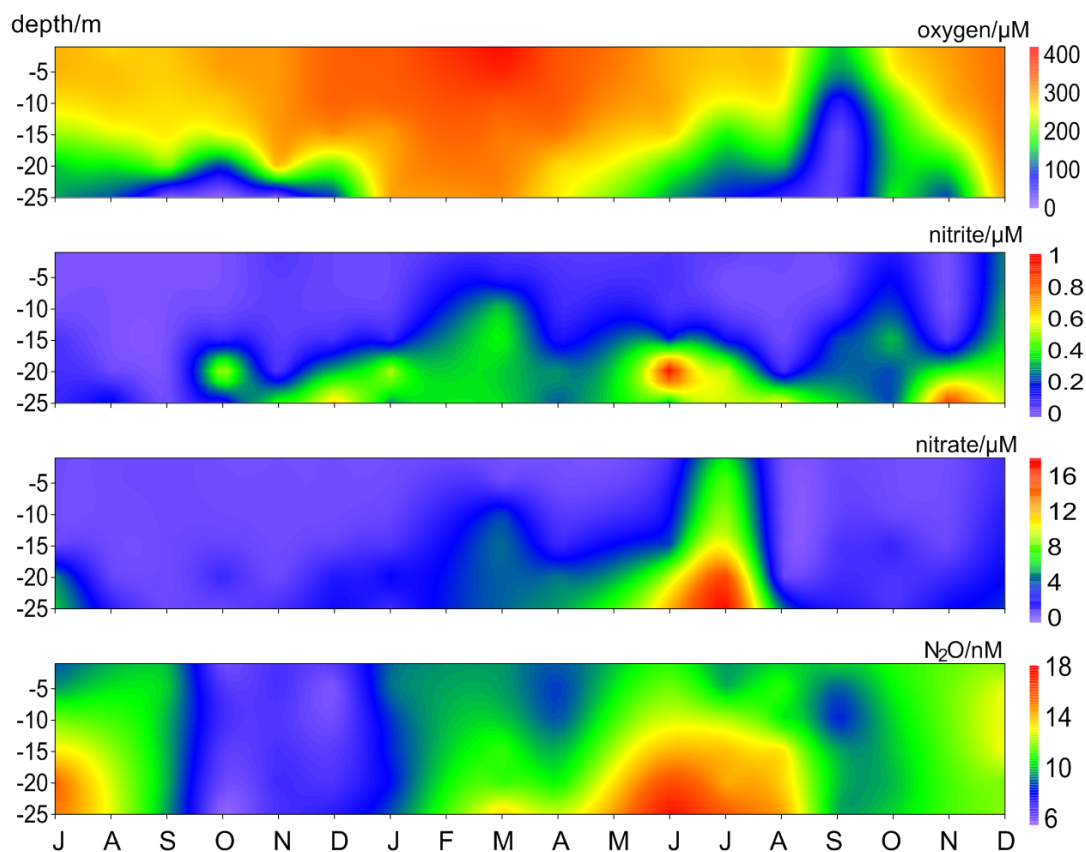
704

Fig. 4 Average vertical distributions of dissolved O_2 , NO_2^- , NO_3^- , and N_2O from the BE Time-Series Station during 2005–2017. The black line indicates the mixed layer depth, which was calculated based on a potential density anomaly of 0.15 kg m^{-3} from the sea surface (1m).



705

706 Fig. 5 Correlation between pH and N₂O concentrations in December, January and February during 2005–2017.



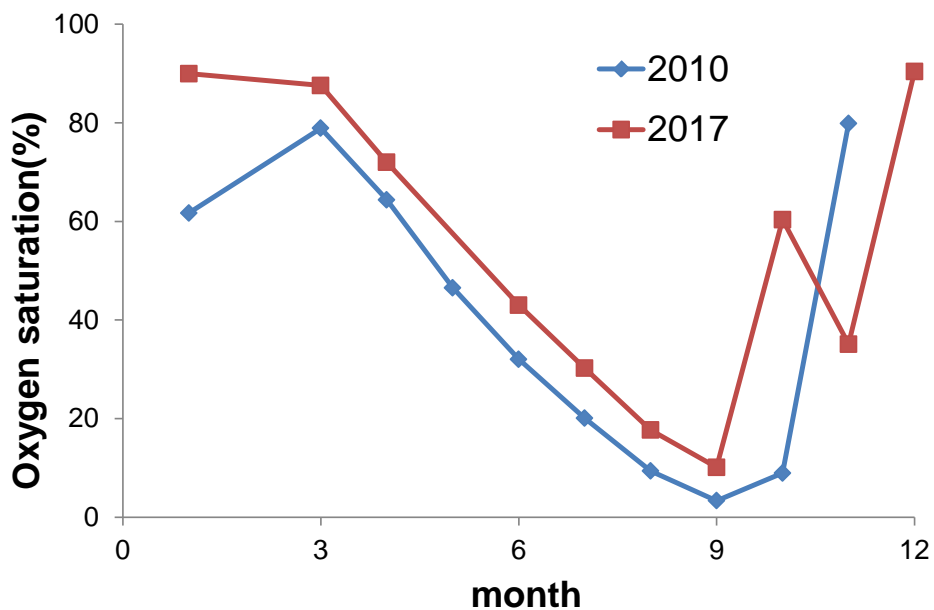
707

708

709

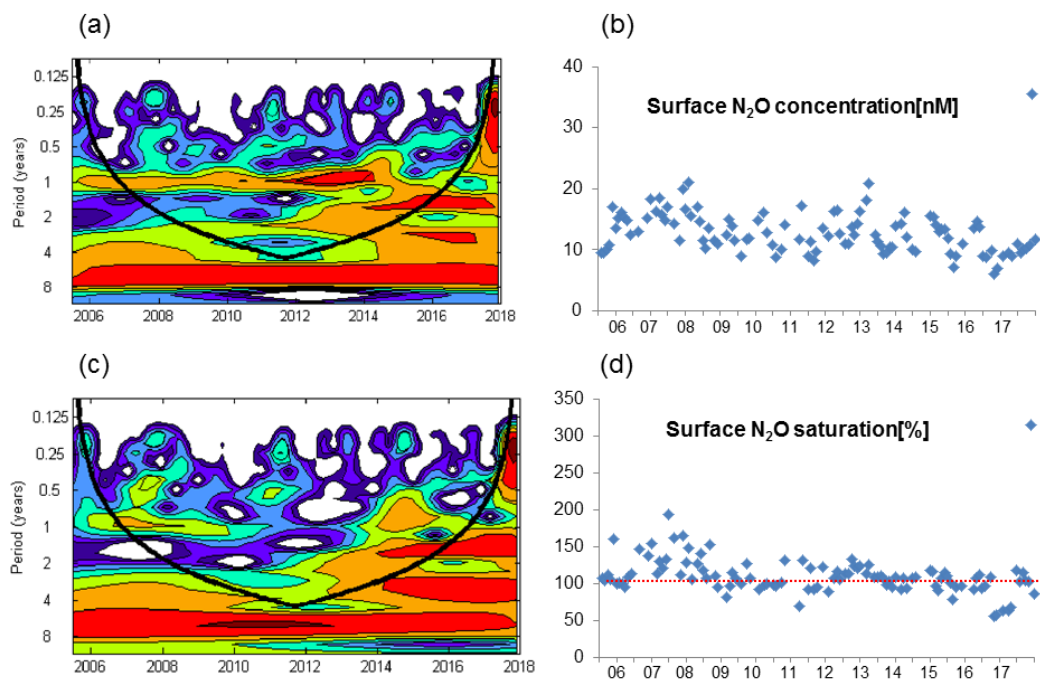
710

Fig. 6 Vertical distribution of dissolved O_2 , NO_2^- , NO_3^- , and N_2O from the BE Time-Series Station during July 2016–December 2017. Please note that the high N_2O concentrations in November 2017 were removed for better visualization.



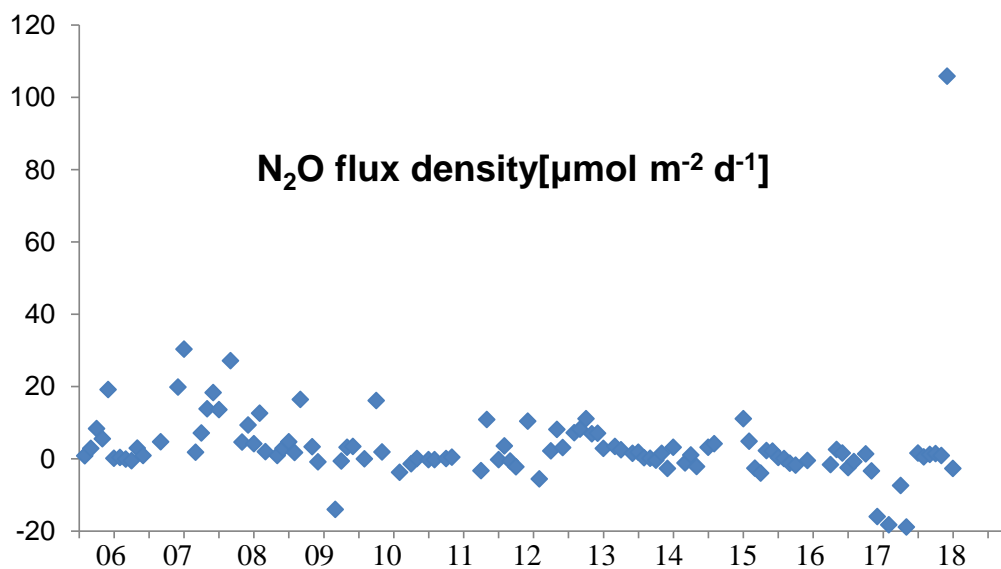
711

712 Fig. 7 Variations of bottom O₂ saturation in 2010 (blue) and 2017 (red).



713

714 Fig. 8 Wavelet analysis and the variation of surface N₂O concentrations (a, b) and surface N₂O saturations (c,
715 d). The dashed red line in (d) indicates the saturation of 100%.



716

717 Fig. 9 Variation of N₂O flux density at the BE Time Series-Station during 2005–2017. Negative values
718 indicated N₂O influx from the atmosphere and positive values indicated N₂O efflux to the atmosphere.